Journal of Applied Fluid Mechanics, Vol. 17, No. 5, pp. 1027-1038, 2024.
Available online at www.jafmonline.net, ISSN 1735-3572, EISSN 1735-3645.
https://doi.org/10.47176/jafm.17.05.2326

Manipulation of Supersonic Jet using Grooved Tabs

A. K. Mali[1], T. Jana[2], M. Kaushik [1†] and S. Thanigaiarasu[3]

[1] *Department of Aerospace Engineering, Indian Institute of Technology, Kharagpur – 721302, India*
[2] *Department of Aerospace Engineering, B.M.S. College of Engineering, Bengaluru - 560019, India*
[3] *Department of Aerospace Engineering, MIT Campus, Anna University, Chennai – 600044, India*

†Corresponding Author Email: mkaushik@aero.iitkgp.ac.in

ABSTRACT

This study experimentally evaluated the mixing augmentation of twin tabs mounted along a diameter at the outlet of a convergent-divergent Mach 1.62 circular nozzle. The usefulness of the plain and grooved tabs is examined at various expansion levels prevailing at nozzle outlet. The tab's performance is assessed through pitot pressure distribution measured along and perpendicular to the jet centerline at different nozzle pressure ratios (NPRs). The shadowgraph technique visualized the shocks and expansion fans in uncontrolled and controlled jets. With the introduction of uncorrugated or plain tabs at the nozzle outlet operating under overexpanded conditions corresponding to NPR 4, the supersonic length (SL) was decreased only by 35.4%. On the other hand, the corrugated or grooved tabs under similar conditions decreased the SL substantially. Interestingly, the performance of grooved tabs was best at underexpanded conditions associated with NPR 6, where the SL was reduced by about 88%. The pressure profiles also established the superiority of tabs with grooved edges in mixing augmentation without introducing any significant asymmetry to the flow field. In addition, the Shadowgraph images also confirmed the weakening of shock strength and reduction of shock-cell length in the case of grooved tabs at the nozzle exit compared to the plain nozzle.

Article History

Received September 18, 2023
Revised December 12, 2023
Accepted December 19, 2023
Available online February 24, 2024

Keywords:

Shock-cell
Supersonic length
Tab
Jet mixing
Flow visualization

1. INTRODUCTION

The investigations on jet mixing characteristics, performed by several researchers, incidentally put forward the concept of tabs. While studying the evolution, aerodynamic mixing, and aeroacoustics noise behavior of jets, primitive researchers were amazed to see the substantial reduction in supersonic length and the sudden disappearance of screech tone with an unplanned insertion of a solid metallic strip into the supersonic length. Since that time, a massive amount of research has been conducted. The subsequent researchers termed the metallic strip, usually placed at the outlet of a nozzle, as a 'Tab' (Fig. 1).

In the mechanical and aerospace industries, jets find several applications. The jet plays a key role in many propulsion and mixing devices, which desire quick and efficient mixing; for example, in ramjets and scramjets, effective mixing is limited by space and time. Additionally, improved mixing of the hot plume from the nozzle with the surrounding fluid suppresses the infrared signature of the exhaust. Other uses include thrust augmentation ejectors, thrust vector control, reducing noise emissions from high-speed jets by creating a low-speed flow region around it (Karabasov, 2010; Kaushik, 2012), etc. Jet mixing has been the focus of several investigations for a long time. The flow development is modified with jet control to fit the intended uses better. The same is accomplished by modifying evolution and creating elements that make up the flow.

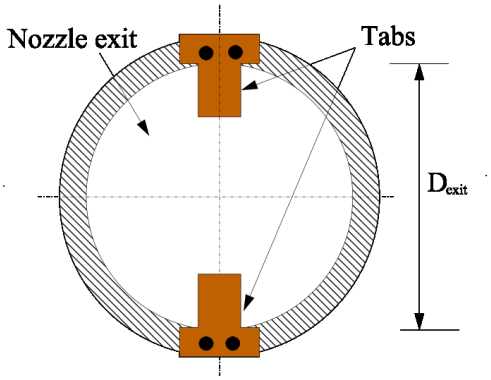

Fig. 1 Schematic view of two diametrically opposite tabs at the nozzle exit

NOMENCLATURE

CPD	Centerline Pressure Distribution	P_{01}	setting chamber pressure
D	nozzle diameter at the outlet	*SL*	Supersonic Length
M	Mach number	*X*	distance along the jet centerline (X-axis)
NPR	Nozzle Pressure Ratio	*Y*	distance normal to the tab direction (Y-axis)
P_{02}	pitot pressure	*Z*	distance along the tab direction (Z-axis)

The compressibility effects and the turbulent shear layer at the jet boundary make mixing high-Speed jets with surrounding fluid very difficult. The shear layer spreading for the compressible jet is up to five times lower than that in the incompressible shear layer (Papamoschou & Roshko, 1988). With the beginning of the first study by Brown and Roshko (1974) on large-scale turbulent structures in supersonic jet mixing promotion, several researchers across the globe proposed different active and passive jet control techniques to achieve the same (Brown & Roshko, 1974).

A jet control makes the flow unstable and sheds large-scale vortices into the flow (Kaushik, 2019; Thangaraj et al., 2022). The commonly used passive controls are the stationary devices in the flow system (such as vortex generators, tabs, etc.) or engraved geometrical modifications (such as non-circular nozzles, grooves, notches, etc.) which alter the shear layer stability characteristics (Kaushik, 2022). Passive control methods employed in the manipulation of supersonic jet dynamics involve not only amplification in the share layer, but also induce modifications to the existing shock cell structure within the supersonic length. Additionally, the effect of passive control techniques can be varied according to the expansion level of the jet. It should be noted that, unlike incompressible jets, Kelvin-Helmholtz instabilities play a much less role in the mixing process due to decreased compressible shear layer growth rate, particularly at supersonic Mach numbers (Martens et al., 1994). However, regarding the mixing efficiency of compressible jets, the streamwise structures are immune to the effects of compressibility in their fast development and entrainment (Tew et al., 2004).

Bradbury and Khadem (1975) were the first who demonstrated the shedding of streamwise vortices by putting tabs 180^0 apart at the nozzle exit and found it advantageous in mixing augmentation (Bradbury & Khadem, 1975). Ahuja and Brown (1989) witnessed identical outcomes for supersonic cold and hot jets; they also saw the alteration in the shock cell structure of the jet with tabs (Ahuja & Brown, 1989). Following this, Zaman et al. (1992, 1994) and Reeder and Samimy (1996) too investigated the characteristics of jets employing tabs (Reeder & Samimy, 1996; Zaman et al., 1992, 1994). Samimy et al. (1993), through their studies, found that the tabs promote mixing only in case of a favorable pressure gradient at the nozzle exit. They also inferred that the streamwise vorticity formation is driven by pressure through an inviscid process rather than by the viscous boundary layer wrapping around the tab (Samimy et al., 1993). The extreme pressure disparity on both the sides of the tab is the primary cause of vorticity formation. From laser sheet visualization, Zaman et al. (1994), Habchi et al. (2010) and Gretta and smith (1993), observed three types of vortices shading from tabs: a pair of oppositely revolving streamwise vortices (a horseshoe vortex) enclosed by separate hairpin vortices, necklace, and trailing-edge vortices (Habchi et al., 2010; Zaman et al., 1994). Compared to hairpin vortices that shed periodically, horseshoe vortices are stationary (Gretta & Smith, 1993). A typical flow field generated by a tab is shown in Fig. 2. The vortices thus produced by the tabs intermix the stagnant surrounding fluid into the high-speed jet, which greatly spreads the turbulent shear layer resulting in enhanced mixing. To investigate further, Hari and Kurian (2001) conducted a quantitative study with primary and secondary tabs at Mach 1.7 circular nozzle exit (Hari & Kurian, 2001). They observed a substantial drop in the supersonic length, an enlarged jet width, and a greater value of shear layer thickness when secondary tabs are mounted along with primary tabs.

Numerous tab configurations, such as tab aspect ratio (Kaushik & Rathakrishnan, 2015), tab corrugation geometries (Behrouzi & McGuirk, 2006; Jana & Kaushik, 2021; Kaushik & Rathakrishnan, 2013), and location of the tabs (Behrouzi & Mcguirk, 1998; Thillaikumar et al., 2020a), have been examined to maximize mixing in supersonic jets. It is established that streamwise vortices produced by different tab configurations aided mixing by increasing the interfacial surface area of the jets as well as the normal gradients to the jet interface. Recently, Thillaikumar et al. (2020a) examined the Mach 1.73 jet mixing characteristics at different expansion levels using tabs with different shapes of grooves, namely, rectangular, semi-circular, and triangular, engraved along tab edges (Thillaikumar et al., 2020b). They revealed that, grooves encouraged mixing more prominently than a plain rectangular tab, reducing the supersonic length. Essentially, grooves generate streamwise vortices, responsible for higher level of mixing. It was seen that the grooves have been very effective when there is a favorable pressure gradient (Kaushik et al., 2006). Later, Ilakkiya and Sridhar (2018) conducted their investigations on the effectiveness of square grooves. They found out that the square groove significantly alters the shock structures. Recent study of Ilakkiya and Sridhar (2022) demonstrated that the grooves of semi-circular shape are very effective in under expanded conditions.

In all the investigations discussed above, it is clear that, though the influence of corrugated shapes over tab is superior in rapid mixing compared to their plain counterparts; however, the impacts of the different corrugation shapes are not much different on jet mixing. Bearing these facts in mind, instead of comparing different corrugations, the current study assesses the performance of tabs with grooves engraved along their edges, called as grooved tabs, installed at the outlet of a Mach 1.62 supersonic circular nozzle (Fig. 3). The plain tab was also

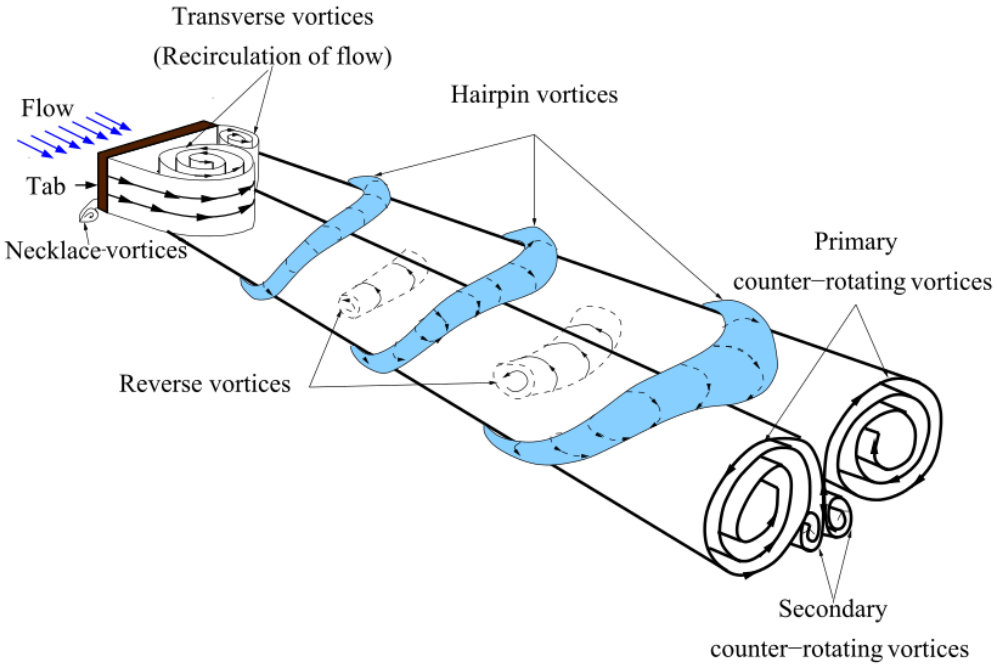

Fig. 2 Schematic of Flow field generated by the tab Grettha and Smith (1993)

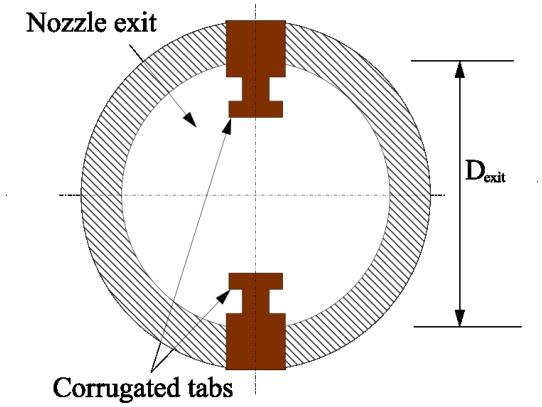

Fig. 3 Graphical representation of the grooved tabs at the circular nozzle outlet plain

studied for comparison. The expansion level at the nozzle exit was changed by changing the nozzle pressure ratio (NPR) from 4 to 8. To reduce the thrust loss, the flow blockages introduced by both plain and grooved tab-pairs were kept at 2.5%. Based on the observation of Lovaraju and Rathakrishnan (2006), and Zaman et al., (1994), which demonstrated that the thrust loss due to the addition of tabs is nearly proportional to the percentage of area obstructed by the tabs, for the present study, the percentage of area blockage by each tab is considered to be 2.5%, which leads to a 2.5% reduction in thrust per tab (Lovaraju & Rathakrishnan, 2006; Zaman et al., 1994).

2. EXPERIMENTAL METHODOLOGY

The experiments were carried out at the Supersonic Jet Research Laboratory, Indian Institute of Technology Kharagpur. The photographic views and schematic of the experimental facility are presented in Fig. 4 and 5, respectively. The pressurized air storage tank, with a capacity of 5000 liters, releases high-pressure dry air that flows via first through cutoff valve and then the pressure control valve. Once the pressure control valve has provided the required air pressure, the pressurized air is next sent into the settling chamber. Subsequently, the pressurized air passes via the test convergent-divergent nozzle, which is fastened with a collar at the other end opening of the settling chamber.

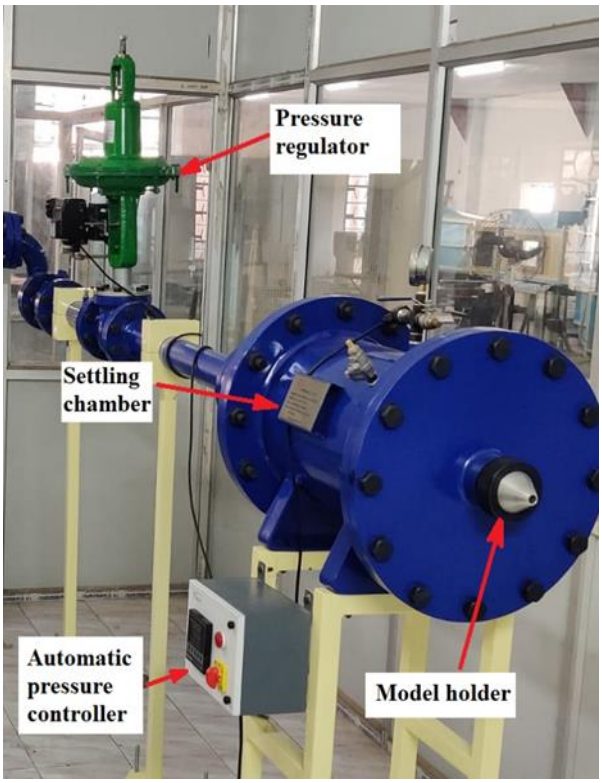

Fig. 4 Photograph of the supersonic jet-test setup at IIT Kharagpur

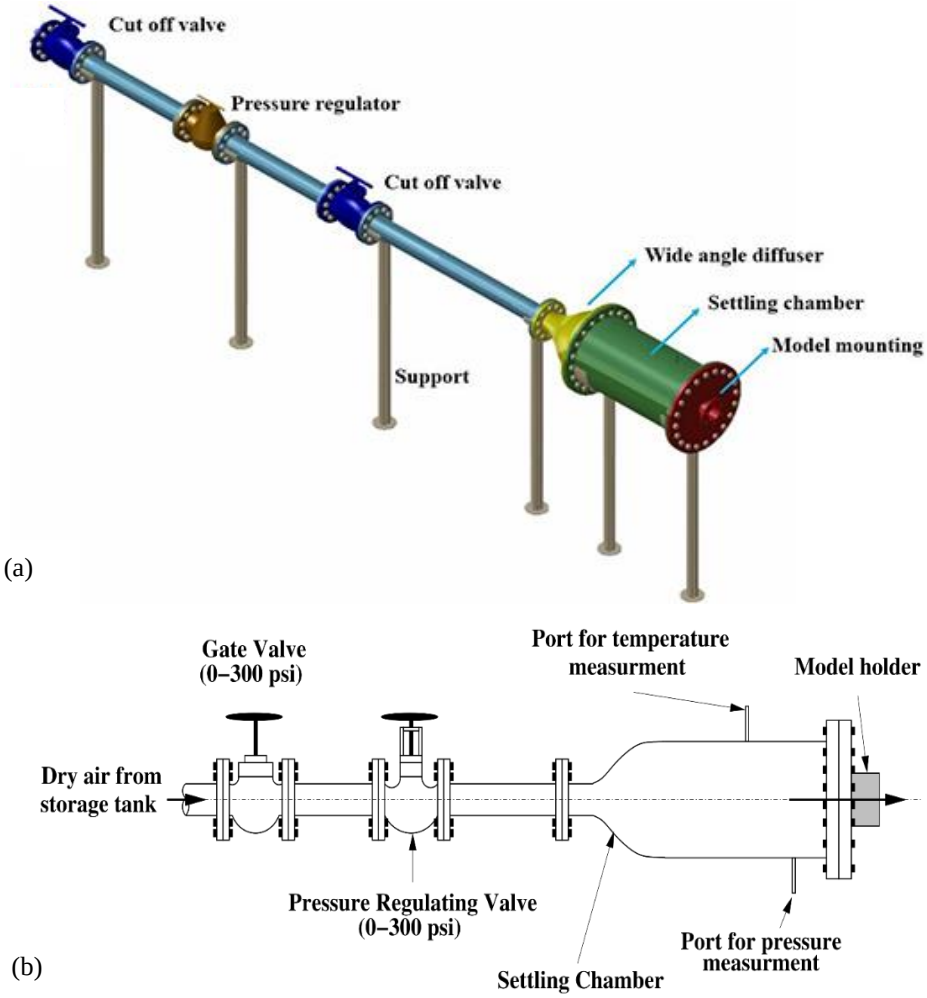

Fig. 5 Schematic representation of the supersonic jet-test setup at IIT Kharagpur

This study measured the stagnation pressure through a Pitot tube fitted on a three-dimensional traverse that has six degrees of freedom (three translational as well as three rotational motions). The traverse has a movable Vernier and a stationary main scale of a translational least count of 0.1 mm and the rotational least count of 1^0. The inner and outer diameters of Pitot tube are 0.4 mm and 0.6 mm, respectively. The ratio of the nozzle outlet area to pitot probe area in the study is 460, a sufficiently higher value to neglect the blockage effect (Kaushik, 2012, 2019). Note that the pressure measured by the Pitot probe is not the total pressure in the supersonic length. Instead, a probe measures the pressure behind the bow shock, which forms ahead of the probe nose in the supersonic flow. The pressure measured behind the bow shock is called the impact pressure.

The Reynolds number considering the nozzle outlet diameter is approximately 5.3×10^5, which is large enough to neglect the viscous effects on Pitot readings. The pitot pressure sensed by the probe was measured using a 16-channel pressure transducer, namely the PSI 9010 type by NUSS pressure Scanner from National Instruments. This transducer was connected to a high-performance computer, which ran VIs-based data gathering software. The Lab VIEW application program establishes a communication link between the host computer and the pressure scanner. The pressure transducer had a sampling frequency of 5000 Hz and an averaging rate of the same value. The transducer has the capability to determine the number of samples to be averaged by utilizing dip-switch settings. As high as 250 samples per second have been recorded and averaged using transducer (Kaushik & Rathakrishnan, 2014). Following the recalibration process, the transducer's accuracy is ±0.15 of the whole scale. Note that, the mean value of pressure is calculated by taking an average of 250 sample data at each point. This transducer was integrated into a data acquisition unit, consisting of a computer installed with manufacturer-provided software. A symmetric nozzle with an exit diameter of 12 mm designed for Mach 1.62 was employed in this investigation. The plain and grooved tabs were fabricated with 1 mm thick brass sheets, with grooves provided at the tab edges. It is important to mention that in order to provide a fair comparison of the effectiveness between plain tabs and square grooved tabs, each tab must have a consistent blockage of 2.5% (of nozzle exit area). As a result, grooved geometries are produced with optimal dimensions, as seen in figure 6. At 1 mm intervals, the impact pressure changes along the jet centerline and in the directions along and perpendicular to the tabs was measured. The shadowgraph technique was used to analyze the shocks and expansion fans present in the supersonic region of the supersonic jet.

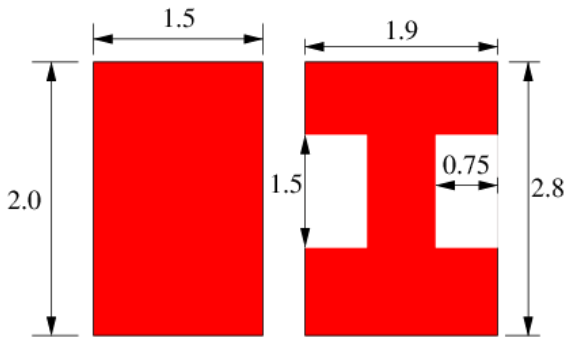

Fig. 6 Graphical views of the plain (uncorrugated) and grooved (corrugated) tabs (All dimensions are in mm)

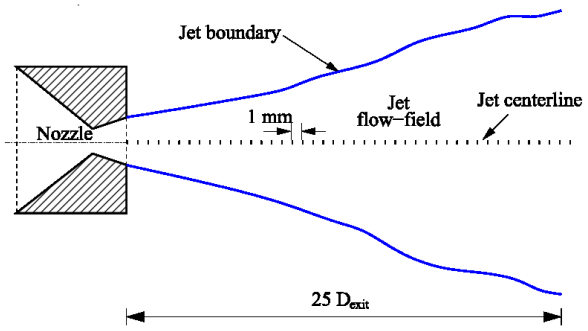

Fig. 7 Measurement stencil, showing axial interval

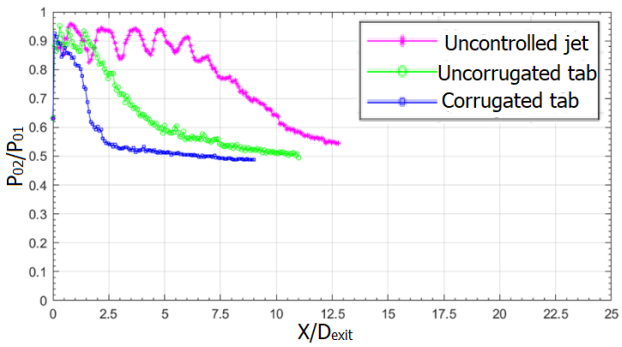

Fig. 8 CPD of Mach 1.62 jet at NPR 4 (overexpanded)

The atmospheric pressure was measured using a mercury barometer with a precision of ± 0.1 mm, or about 0.1%. The pitot probe, which was mounted on a traverse, could move ±0.1 mm in a straight line. The pressure readings fluctuated because the pressure-regulating valve was controlled by a servo motor, which was in turn controlled by a digital controller. The overall error in the pressure measurements was about ± 1%. The uncertainties in the design Mach number, P/P_0, and expansion level were about ±0.05, ±0.05, and ±0.01, respectively. The uncertainty analysis showed that the pressure readings were precise to about ±3%. (Kaushik, 2012).

3. RESULTS AND DISCUSSION

A Pitot tube measures the pressure in the downstream side of a bow shock (P_{02}) formed in its nose region in supersonic or hypersonic flows, which is known as impact pressure. The total pressure in the upstream side of the detached shock may be obtained by incorporating a correction factor due to pressure loss. However, it is well established in the literature that the non-dimensional variations of impact pressure (P_{02}) along and perpendicular to the jet centerline are good enough to understand the jet mixing qualitatively. In this study, P_{02} is made non-dimensional by dividing it with P_{01} (settling chamber stagnation pressure) and plotted against non-dimensional axial (X/D_{exit}) and transverse distances (Y/D_{exit}) and Z/D_{exit}); D_{exit} refers to nozzle exit diameter. Also, the X axis corresponds to the jet centerline, and the Y and Z axes are perpendicular to the jet centerline.

3.1 Centerline Pressure Distribution (CPD)

A Pitot probe obtains the impact pressures along the jet centerline (x-axis) at varied expansion levels. The probe was moved right from the jet exit up to a distance of $25D_{exit}$ in steps of 1 mm along the centerline, as illustrated in Fig. 7. Essentially, the decay in CPD measures the decay of the impact pressure along the jet centerline. The crest and trough in the pressure plot define the SL as it is dominated by shock and expansion waves. A higher jet mixing can ensure by obtaining the lower SL using control techniques. In this section, the CPD for the supersonic uncontrolled jet and the supersonic jet controlled with plain and grooved tabs is compared.

The centerline pressure decays for Mach 1.62 uncontrolled and controlled supersonic jets at the overexpanded level associated to NPR 4 are plotted in Fig. 8. Here, an oblique shock cone is generated at the outlet of the nozzle to level the lower flow outlet pressure with the higher back pressure. It can be seen that both the tab with grooves and the plain tab weaken the powerful waves that are present in the uncontrolled jet. When the jet is over-expanded, the impact of the plain and grooved tabs on the SL reduction are essentially identical. Note that, the axial range till which supersonic flow predominates is considered as the supersonic length (Shirie & Seubold, 1967). It can be observed that the supersonic length for the uncontrolled jet at NPR 4 extends to around $8D_{exit}$. The supersonic length drops to $5D_{exit}$ when plain tabs are employed at the nozzle outlet, while it is only around $3D_{exit}$ when grooved tabs are used. Additionally, the shock cell's strength has been greatly diminished. Essentially, grooved tabs have a greater number of sharp corners than regular plain tabs, resulting in more vortices emanating from these corners compared to plain tabs consequently, a greater interaction between jet fluid and the surrounding fluid.

At NPR 5, the SL of plain and controlled jets controlled with plain and grooved tabs are $12.5D_{exit}$, $5D_{exit}$, and $3D_{exit}$, respectively, as shown in Fig. 9. The tabs, however, considerably reduce the strength of the shock and expansion fans in the supersonic length. Additionally, it has been observed that the plain tab works better than the grooved tab at dampening the waves. Note that, the plain tab's characteristic decay is similar to that of an uncontrolled jet while the grooved tab's characteristic decay is quicker.

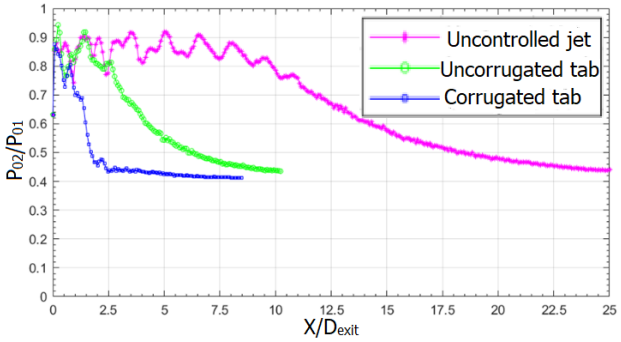

Fig. 9 CPD of Mach 1.62 jet at NPR 5 (correctly-expanded)

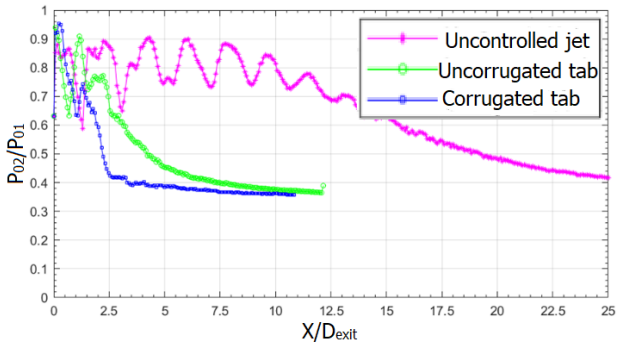

Fig. 10 CPD of Mach 1.62 jet at NPR 6 (underexpanded)

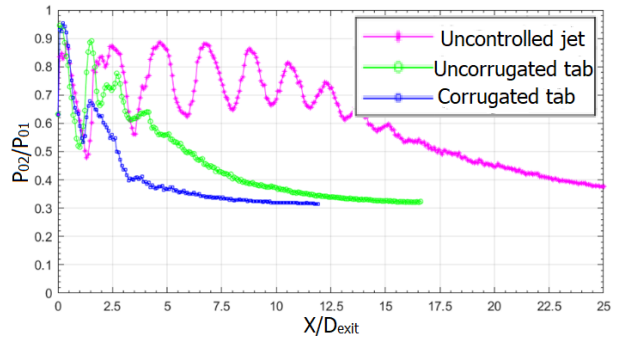

Fig. 11 CPD of Mach 1.62 jet at NPR 7 (underexpanded)

Figure 10 demonstrates that plain and grooved tabs have entirely different impacts at NPR 6. In the supersonic length, typical decay, and far field zones, the grooved tab promotes mixing more effectively than the plain tab. NPR 6 shows a case of underexpansion, in which the SL of a supersonic jet from an uncontrolled nozzle is 17Dexit. The most significant reduction in the SL occurs when grooved tabs are employed at NPR 6, resulting in a length of supersonic region is $2.2D_{exit}$. The CPD plot clearly shows a notable reduction in the number of shock cells within the supersonic region when grooved tabs are utilized. Specifically, the implementation of grooved tabs results in a decrease from nine shock cells in an uncontrolled jet to two shock cells. As illustrated in Fig. 11, apart from the near field region, the grooved tab's efficiency is higher than the plain tab at NPR 7 which corresponds to higher

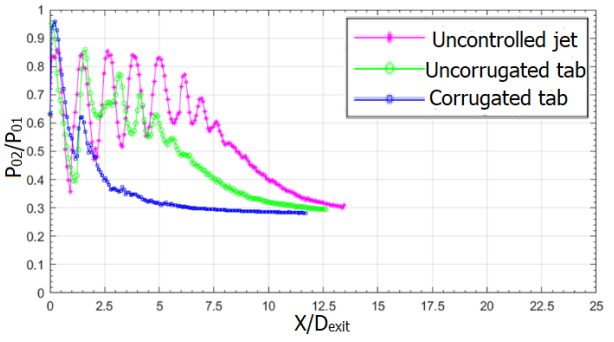

Fig. 12 CPD of Mach 1.62 jet at NPR 8 (highly underexpanded)

advantageous pressure gradient at the nozzle outlet. Figure 11 also demonstrates that the intensity of the initial shock cell remains consistent in both plain and controlled jets. Additionally, it is apparent that grooved tabs exhibit superior performance compared to plain tabs following the initial shock cell. The SL for jets with grooved tabs are $3D_{exit}$, whereas, for jets with plain tabs, it is $5D_{exit}$. Figure 12 displays the CPD graphs for both controlled and uncontrolled jets at the under-expanded level corresponding to NPR 8. With the exception of the characteristic decay zone, the plain and grooved tabs functioned nearly identically. It is clear from Fig. 11 and 12 that at NPRs 7 and 8, the grooved tab's supersonic length waves are weaker than those of the plain tab. However, one noticeable difference between NPR 7 and NPR 8 is that NPR 8 shows larger fluctuations in CPD than NPR 7. The reason for this phenomenon lies in the fact that a higher positive pressure gradient serves to augment the intensity of the shock cell. Moreover, it can be noted that the SL for NPR 8 is significantly shorter compared to NPR 7. Specifically, for an uncontrolled jet, the SL for NPR 8 measures $8D_{exit}$, whereas for NPR 7, it measures $17D_{exit}$. The supersonic length prevails till $8D_{exit}$ at NPR 8 for both the uncontrolled jet and the plain tab. However, for grooved tabs, the SL is reduced to $2.5D_{exit}$, demonstrating a significant improvement over uncontrolled jet. Therefore, placing grooves across tab edges at the under-expansion levels proved to be quite advantageous compared to their plain counterpart.

The comparison of the SL reduction for the plain and grooved tabs is shown in Table 1. At all tested NPRs, it can be seen that the grooved tab has a smaller jet SL than the plain tab.

Different SL reductions at various NPRs are plotted in Fig. 13. It can be seen that the grooved tab at NPR 6 achieves the maximum SL reduction of 88%. As can be

Table 1 Reduction in SL at various NPRs

NPR	Plain tab (%)	Grooved tab (%)
4	35.4	60.4
5	19.3	75.7
6	14.5	88
7	7.1	85.4
8	32.5	67

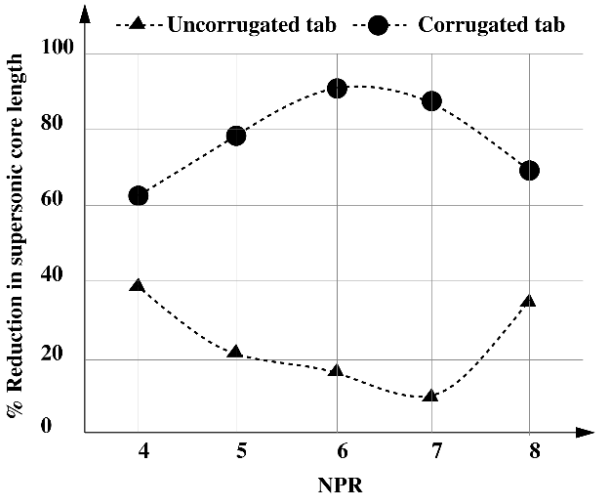

Fig. 13 Variation in SL with NPR for Mach 1.62 jet

observed in Fig.12, the trend for the reduction in the SL with NPR for plain tab and the grooved tab are quite different. For plain tab, the maximum reduction in SL can be observed at NPR 4 and NPR 8. On the other hand, for grooved tab the SL reduction is maximum at NPR 6, further increase of which decreases the grooved tab efficiency. However, for all the NPRs, grooved tabs perform better than the plain tab in reducing the SL.

Essentially, the results demonstrate that the level of expansion at the nozzle exit as well as the grooves provided at the tab's edges substantially influence the effectiveness of the tabs. From the perspective of mixing promotion, the tab that creates smaller vortices over a longer radial location at the nozzle outlet has been found to be advantageous. Essentially, due to the implementation of grooved geometries over the tabs, comparatively smaller vortices of varying size have been generated. These additional varying sized mixing promoting vortices are responsible for the higher rate of jet mixing.

3.2 Pressure Profiles

As the control surfaces are introduced in order to manipulate the supersonic length, it introduces flow asymmetry. Therefore, the concentration needs to be provided in reducing flow asymmetry while manipulating the supersonic length. The measured impact pressure distributions are plotted in both Y (normal to the tab) and Z (along the tab) directions, as shown in Fig. 14, to evaluate the asymmetry caused by the grooved and plain tabs.

The radial impact pressure variations for the Mach 1.62 jet at the overexpanded condition, correspond to NPR 4, demonstrate the symmetric profile of the uncontrolled jet, as shown in Fig. 15. However, the controlled jet with an plain tab has significant y and z asymmetry. Interestingly, when the grooves are introduced, the asymmetry in the flow field has significantly decreased due to the mixed size of the streamwise vortices that are shed by the grooved tab. The spread of the jet in both the y and z directions is nevertheless constrained by the interaction of the mixed-size vortices. Note that, the

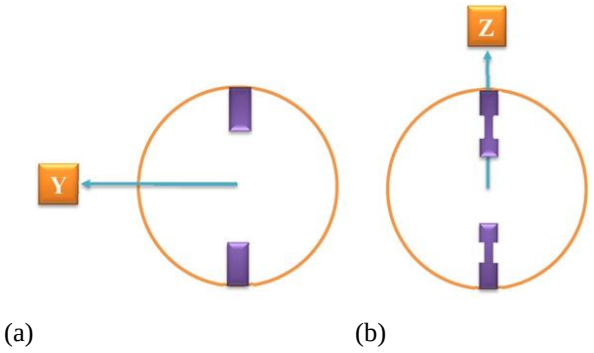

Fig. 14 Schematic views of (a) normal to tab (y-profile) (b) along the tab (z-profile) directions

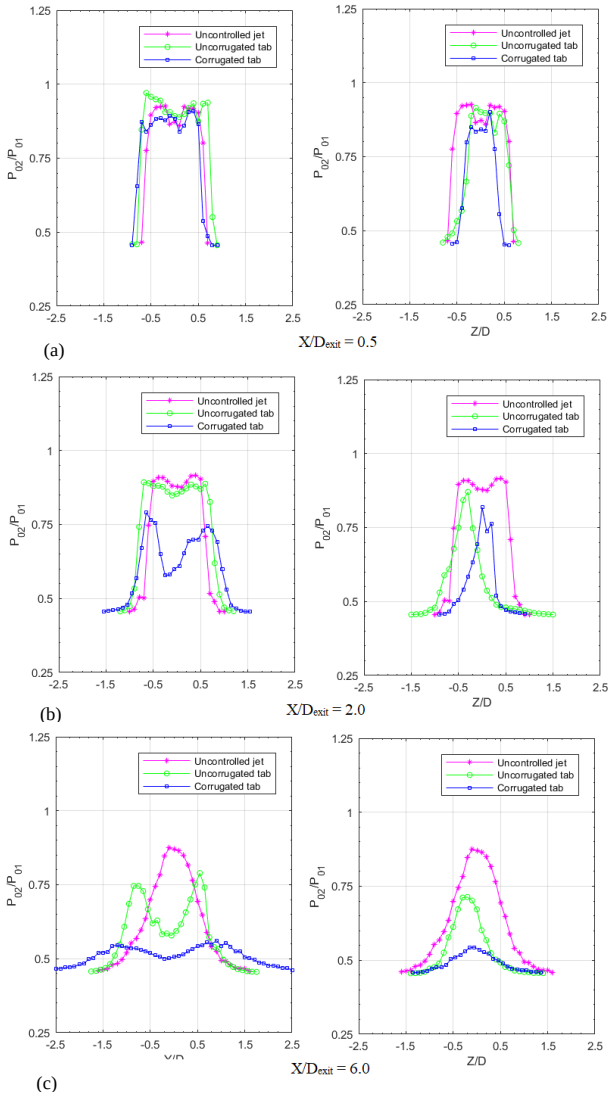

Fig. 15 Radial Pressure Plots of Mach 1.62 jet at NPR 4 (overexpanded)

spread rate for grooved tab is maximum when viewed perpendicular to the tab. However, when viewed along the tab, the spread rate is minimum for the grooved tab. Furthermore, the plain tab introduces greater asymmetry in the both near field and in the far field, whereas the grooved tab performed equally well in the far field than

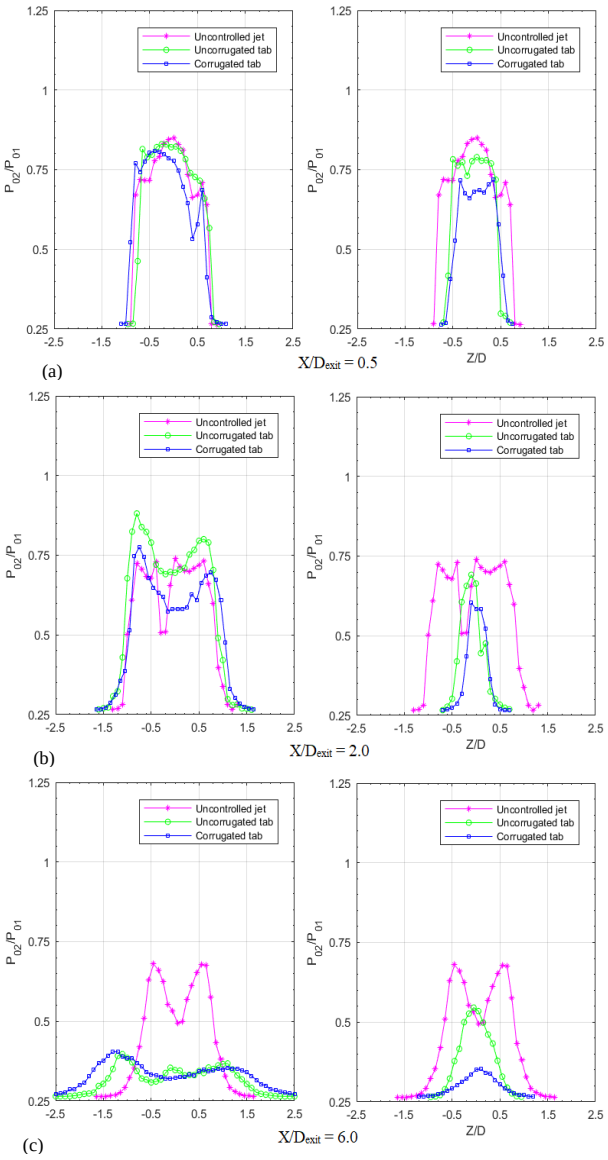

Fig. 16 Radial Pressure Plots of Mach 1.62 jet at NPR 8 (highly under-expanded)

that of near field. It is important to note that, the nearfield location of the supersonic jet, as seen in Figures 14(a) and 15(a), are not much effected by grooved tabs in reducing the asymmetry. However, the far field locations, as demonstrated by Figs 14(b-c) and 15(b-c), are showing the superiority of the grooved tab in reducing the asymmetry when compared it with plain tab. The jet decay at the far field location is far higher for the grooved tab-controlled jet than that for plain tab controlled and uncontrolled jets.

From Fig. 16, it can be observed that, the grooved tab lessens the asymmetry in the z-direction for the underexpanded jet state corresponding to NPR 8, whereas, the plain tab significantly augments asymmetry in the z-profile. Jet spreading rate for plain tab is observed to be greater than that for grooved tab along the z direction. However, at the far field, jet decay for the grooved tab found to be the highest in both the y and z direction. It can be noted that, for both the near-field and far-field regions at this NPR, the grooved tab has continued to be superior to the plain tab in restoring symmetry.

3.3 Optical Flow Visualization

An analysis of the jet flow domain is conducted by examining shadowgraph pictures captured by a high-resolution 1080p DLSR 24 MP camera. The purpose is to validate the observations and conclusions about the CPD and radial pressure profiles, by comparing the images acquired with and without controls. Figure 17(a) depicts the waves in the plain jet at NPR 4. There are two oblique shocks at the nozzle outlet, and they crossover each other and get reflected as expansion fans at the jet's inner boundary. The shock cell is essentially the distance from one crossover point to the nearest crossover point. When the plain tab is implemented into the flow domain, the shock cell pattern of the supersonic jet gets altered, which can be observed in Fig. 17(b) (viewed normal to and tab-along directions). Besides, the introduction of plain tabs results in a modification of the jet width. When the visualization is conducted along the tabs, the width of the jet is found to be higher; however, when viewed perpendicular to the tabs, the width of the jet is lower in comparison with the uncontrolled jet width.

Additionally, when considering the controlled jet with plain tabs, the first crossover point of the wave is observed to be situated at a comparably greater distance downstream than an uncontrolled jet. The shocks and expansion fans pattern in the jet controlled with grooved tab, in both directions are shown in Fig. 17(c). Through a comparative analysis of the shadowgraph visualizations of jets of plain and grooved tabs, it becomes evident that the presence of corrugation introduces additional shock structures in the flow. These additional shock structures, exhibit a lesser strength compared to the undisturbed shock-cell pattern visible in the uncontrolled jet.

The shocks and expansion fans in an uncontrolled jet are seen in Fig. 18(a) for the jet with highly underexpanded conditions associated with NPR 8. The wave of higher strength demonstrates the typical characteristics of a supersonic jet at highly underexpanded conditions. In this situation, the occurrence of regular reflection of the intercepting shock is no longer possible on the axis, as can be observed in Fig. 18(a). Consequently, this reflection becomes singular and gives rise to the formation of a normal shock wave, normally called as the Mach disc. The wave patterns in the jet controlled with an plain tab are displayed in Fig. 18(b). Employing plain tabs for jet control leads to a noticeable strengthening of the first shock cell.

In contrast, successive shock cells farther downstream undergo diminution, as shown by the measured fluctuations in CPD. For the grooved tab, the shocks and expansion fans present in the jet field in the directions perpendicular to and along the tab are shown in Fig. 18(c). The effect of grooved tabs on underexpanded jets is the same as in plain tabs up to the first shock cell. In addition to that jet experience, additional expansion waves were detected near the first shock cell. The collective effect of this phenomenon leads to several alterations in downstream shock cell structure.

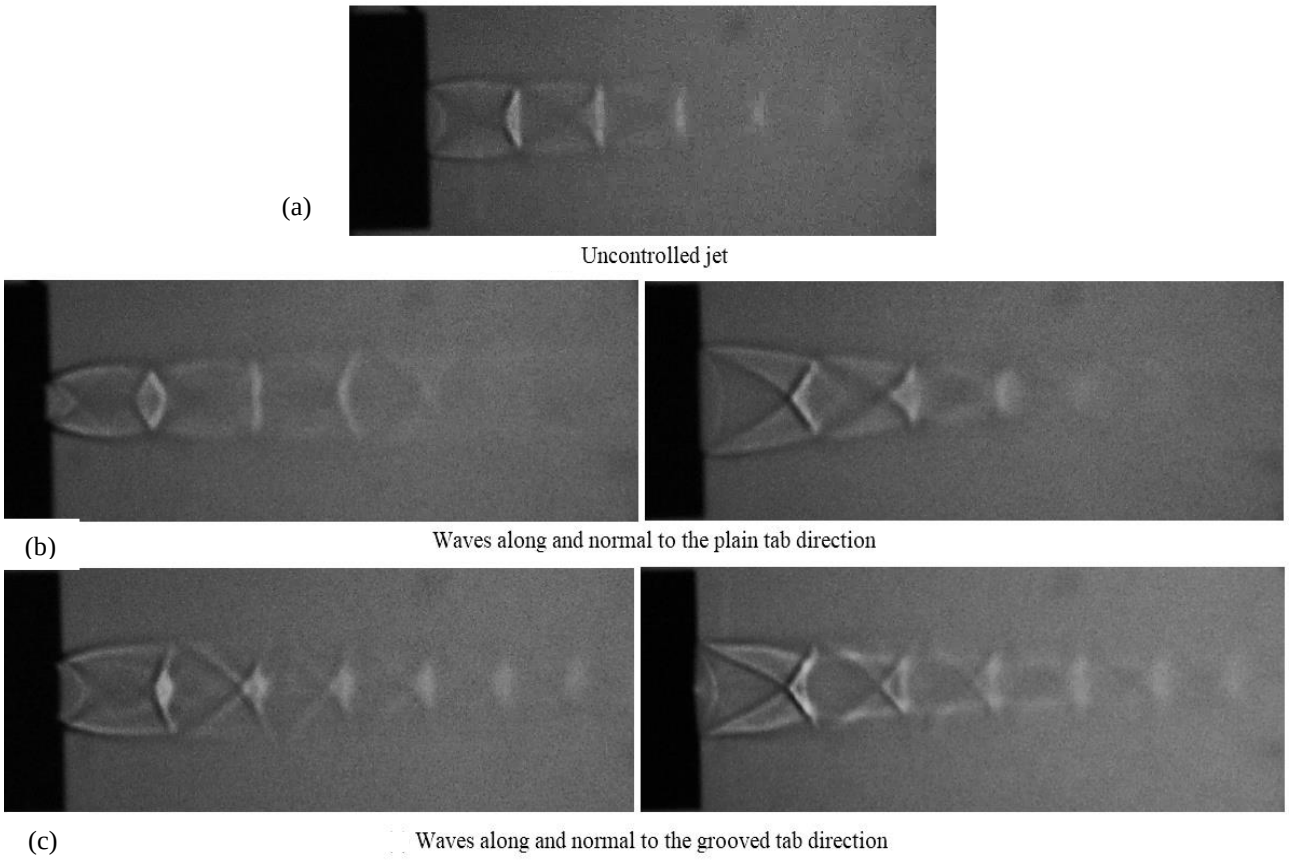

Fig. 17 Shadowgraphic flow visualization for Mach 1.62 jet at NPR 4 (over-expanded)

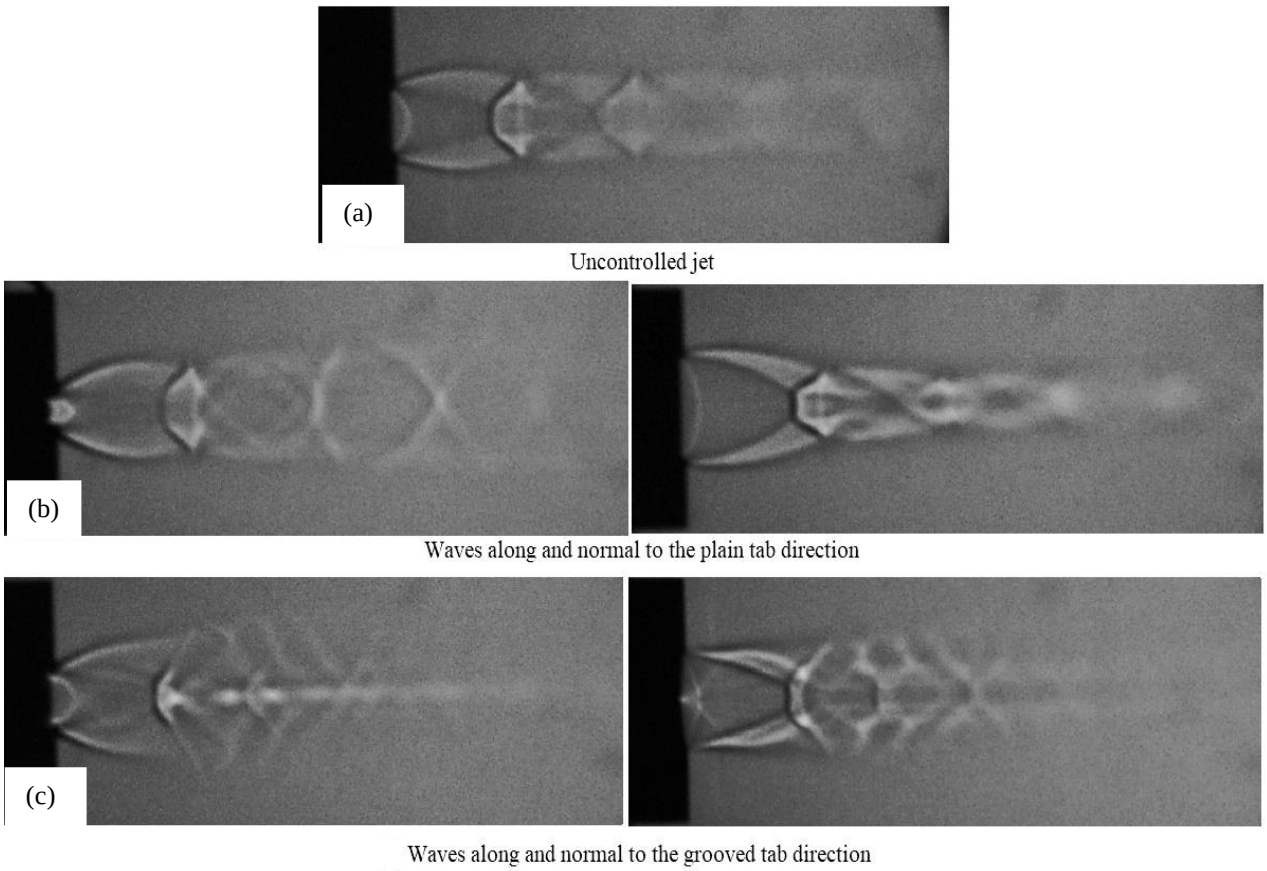

Fig. 18 Shadowgraphic flow visualization for Mach 1.62 jet at NPR 8 (highly underexpanded)

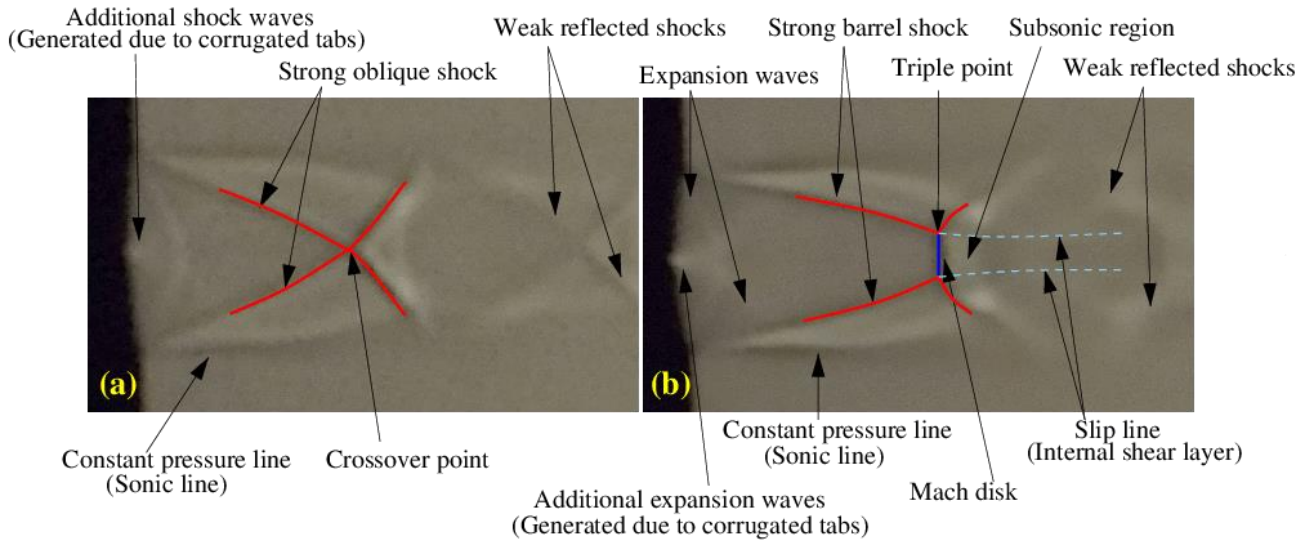

Fig. 19 Jet nearfield flow structures with grooved tabs for (a) overexpanded, and (b) underexpanded condition

In addition to the above Shadowgraphic visualization analysis, Fig. 19(a) and (b) compares the jet with grooved tabs for overexpanded and underexpanded jets to better understand the altered shock wave structure. Irrespective of the expansion condition of the jet at the outlet of the nozzle, expansion waves are formed at the exit of the nozzle due to the sudden relaxation of the flow from the nozzle exit. These expansion waves are reflected from the constant pressure line as shock waves. Furthermore, the existence of grooved tabs at the nozzle outlet leads to additional shock waves formation along the edges of the grooved tabs. The collaborative effect of these two phenomena results in the development of a strong oblique shock in the case of an overexpanded jet, which is clearly shown in fig. 19(a). Furthermore, the intersection occurs downstream distance precisely on the central axis of the jet, where two incoming oblique shocks converge, called the cross-over point. At the crossover point, like reflection occurs, thereby a strong oblique shock is reflected as the same. When these strong oblique shocks incident on a constant pressure line, unlike reflection occurs and the oblique shock gets converted into expansion waves. The jet flow gets further decelerated for grooved tabs in comparison with jet flow with plain tabs because of these strong oblique shocks, which ultimately affect downstream flow conditions and shock structures get weakened.

In an underexpanded jet case, the exit jet flow pressure is much greater than that of the surrounding pressure, which results in the development of expansion waves at the nozzle outlet. Because of the presence of grooved tabs at the nozzle exit, more expansion waves are formed at the edges of the grooves. In addition to that, due to flow relaxation, further Prandtle-Mayer expansion waves are created at the nozzle leap. These expansion waves impinge on a constant pressure line and get reflected as a shock wave. These reflected shock waves converged to form a strong barrel shock. This strong barrel shock meets at the first crossover point and forms the Mach disk, which is clearly visible in Fig. 19(b). The point where the three shocks meet, namely the incident shock (barrel shock), the reflected shock, and a Mach stem (Mach disk), is called the triple point, which is also clearly seen in Fig. 19(b). In the region immediately after the Mach disc, the flow velocity is seen to be below the speed of sound, indicating a subsonic state inside that particular isolated area. In order to separate the subsonic flow from the external supersonic flow, a distinct internal shear layer, commonly referred to as a slip line, is established. The collaborative effect of all these phenomena in an underexpanded jet results in the alteration and weakening of the shock cell structure in the downstream flow and the mixing of the flow.

4. CONCLUSION

The pressure distributions and Shadowgraphic images from the investigation show that the tab with grooves is more effective at lowering the SL than the plain tab. The SL reductions for plain and grooved tabs are 35.4% and 60.4%, respectively, when the jet is overexpanded, but they are 19.3% and 75.7% when the jet is correctly expanded. The SL decrease caused by the grooved tab is 88% at an underexpanded state associated with NPR 6. As a result, the plain tab effectively lowered the SL when it was overexpanded. In contrast, the greater performance of the grooved tab was demonstrated when the jet was underexpanded. The pressure profiles indicate that the grooved tabs cause rapid mixing while producing no discernible asymmetry in the jet cross-section. The shadowgraph photographs highlight the benefits of grooved tabs by shortening the shock-cell pattern and lowering the shock strength.

CONFLICT OF INTEREST

Authors declare a no conflict of interests.

AUTHORS CONTRIBUTION

A. K. Mali investigated the problem and analyzed the data. **T. Jana** wrote the first draft. **M. Kaushik** supervised

the study and revised the first draft. **S. Thanigaiarasu** reviewed and edited the final version.

REFERENCES

Ahuja, K. K., & Brown, W. H. (1989). Shear flow control by mechanical tabs. *AIAA 2nd Shear Flow Conference, 1989*. https://doi.org/10.2514/6.1989-994

Behrouzi, P., & Mcguirk, J. J. (1998). Experimental studies of tab geometry effects on mixing enhancement of an axisymmetric jet. *JSME International Journal Series B*, *41*(4), 908–917. https://doi.org/10.1299/jsmeb.41.908

Behrouzi, P., & McGuirk, J. J. (2006). Effect of tab parameters on near-field jet plume development. *Journal of Propulsion and Power*, *22*(3), 576–585. https://doi.org/10.2514/1.15473

Brown, G. L., & Roshko, A. (1974). On density effects and large structure in turbulent mixing layers. *Journal of Fluid Mechanics*, *64*(4), 775–816. https://doi.org/10.1017/S002211207400190X

Gretta, W. J., & Smith, C. R. (1993). The flow structure and statistics of a passive mixing tab. *Journal of Fluids Engineering, Transactions of the ASME*, *115*(2), 255–263. https://doi.org/10.1115/1.2910133

Habchi, C., Lemenand, T., Valle, D. Della, & Peerhossaini, H. (2010). Turbulence behavior of artificially generated vorticity. *Journal of Turbulence*, *11*(November 2020), 1–10. https://doi.org/10.1080/14685248.2010.510841

Hari, S., & Kurian, J. (2001). Effectiveness of secondary tabs for supersonic mixing. *Experiments in Fluids*, *31*(3), 302–308. https://doi.org/10.1007/s003480100285

Ilakkiya, S., & Sridhar, B. T. N. (2018). An experimental study on the effect of square grooves on decay characteristics of a supersonic jet from a circular nozzle. *Journal of Mechanical Science and Technology*, *32*(10), 4721–4729. https://doi.org/10.1007/s12206-018-0919-9

Ilakkiya, S., & Sridhar, B. T. N. (2022). Study of decay, spread, and shock structure of a supersonic jet issuing from a C-D nozzle with semi-circular grooves. *Thermophysics and Aeromechanics*, *29*(3), 327–346. https://doi.org/10.1134/S0869864322030027

Jana, T., & Kaushik, M. (2021). Performance of corrugated actuator-tabs of aspect ratio 2.0 on supersonic jet mixing enhancement. *Journal of Mechanical Science and Technology*, *35*(3), 1087–1097. https://doi.org/10.1007/s12206-021-0222-z

Karabasov, S. A. (2010). Understanding jet noise. *Philosophical Transactions of the Royal Society A: Mathematical, Physical and Engineering Sciences*, *368*(1924), 3593–3608. https://doi.org/10.1098/rsta.2010.0086

Kaushik, M. (2012). *Innovative passive control techniques for supersonic jet mixing* (1 st ed.). Lambert Academic Publishing.

Kaushik, M. (2019). *Theoretical and experimental aerodynamics* (1st ed.). Springer Singapore. https://doi.org/10.1007/978-981-13-1678-4

Kaushik, M. (2022). *Fundamentals of gas dynamics* (1st ed). Springer Singapore. https://doi.org/10.1007/978-981-16-9085-3

Kaushik, M., & Rathakrishnan, E. (2013). Corrugated limiting tab for jet mixing. *International Journal of Turbo and Jet-Engines*, *30*(4), 359–373. https://doi.org/10.1515/tjj-2013-0016

Kaushik, M., & Rathakrishnan, E. (2014). Corrugated tabs for supersonic jet mixing. *International Review of Mechanical Engineering*, *8*(6), 983–991. https://doi.org/10.15866/ireme.v8i6.4756

Kaushik, M., & Rathakrishnan, E. (2015). Tab aspect ratio effect on supersonic jet mixing. *International Journal of Turbo & Jet-Engines*, *32*(3), 265–273. https://doi.org/10.1515/tjj-2014-0032

Kaushik, M., Thakur, P. S., & Rathakrishnan, E. (2006). Studies on the Effect of Notches on Circular Sonic Jet Mixing. *Journal of Propulsion and Power*, *22*(1), 211–214. https://doi.org/10.2514/1.8424

Bradbury, L. J. S., & Khadem, A. H. (1975). The distortion of a jet by tabs. *Journal of Fluid Mechanics*, *70*(4), 801–813. https://doi.org/10.1017/S0022112075002352

Lovaraju, P., & Rathakrishnan, E. (2006). Subsonic and transonic jet control with cross-wire. *AIAA Journal*, *44*(11), 2700–2705. https://doi.org/10.2514/1.17637

Martens, S., Kinzie, K. W., & McLaughlin, D. K. (1994). Measurements of Kelvin-Helmholtz instabilities in a supersonic shear layer. *AIAA Journal*, *32*(8), 1633–1639. https://doi.org/10.2514/3.12153

Papamoschou, D., & Roshko, A. (1988). The compressible turbulent shear layer: an experimental study. *Journal of Fluid Mechanics*, *197*(1973), 453–477. https://doi.org/10.1017/S0022112088003325

Reeder, M. F., & Samimy, M. (1996). The evolution of a jet with vortex-generating tabs: Real-time visualization and quantitative measurements. *Journal of Fluid Mechanics*, *311*, 73–118. https://doi.org/10.1017/S0022112096002510

Samimy, M., Zaman, K. B. M. Q., & Reeder, M. F. (1993). Effect of tabs on the flow and noise field of an axisymmetrie jet. *AIAA Journal*, *31*(4), 609–619. https://doi.org/10.2514/3.11594

Shirie, J. W., & Seubold, J. G. (1967). Length of the supersonic core in high-speed jets. *AIAA Journal*, *5*(11), 2062–2064. https://doi.org/10.2514/3.4369

Tew, D. E., Hermanson, J. C., & Waitz, I. A. (2004). Impact of compressibility on mixing downstream of

lobed mixers. *AIAA Journal*, *42*(11), 2393–2396. https://doi.org/10.2514/1.11004

Thangaraj, T., Kaushik, M., Deb, D., Unguresan, M., & Muresan, V. (2022). Survey on vortex shedding tabs as supersonic jet control. *Frontiers in Physics*, *9*(February), 1–17. https://doi.org/10.3389/fphy.2021.789742

Thillaikumar, T., Bhale, P., & Kaushik, M. (2020a). Experimental investigations on the strut controlled thrust vectoring of a supersonic nozzle. *Journal of Applied Fluid Mechanics*, *13*(4), 1223–1232. https://doi.org/10.36884/JAFM.13.04.31069

Thillaikumar, T., Jana, T., & Kaushik, M. (2020b). Experimental assessment of corrugated rectangular actuators on supersonic jet mixing. *Actuators*, *9*(3), 1–24. https://doi.org/10.3390/act9030088

Zaman, B., Reeder, M., & Samimy, M. (1992, July 6). *Supersonic jet mixing enhancement by "delta-tabs."* 28th Joint Propulsion Conference and Exhibit. https://doi.org/10.2514/6.1992-3548

Zaman, K. B. M. Q., Reeder, M. F., & Samimy, M. (1994). Control of an axisymmetric jet using vortex generators. *Physics of Fluids*, *6*(2), 778–793. https://doi.org/10.1063/1.868316